PRAMANA
— journal of
physics

© Indian Academy of Sciences

Vol. 61, No. 6
December 2003
pp. 1121–1128

# Optimization of soft x-ray line emission from laser-produced carbon plasma with laser intensity

A CHOWDHURY, R A JOSHI, G P GUPTA*, P A NAIK and P D GUPTA
Laser Plasma Division, Centre for Advanced Technology, Indore 452 013, India
*Laser and Plasma Technology Division, Bhabha Atomic Research Centre, Mumbai 400 085, India
Email: avijit@cat.ernet.in

MS received 11 March 2003; accepted 3 July 2003

**Abstract.** Absolute measurement for He-$\alpha$ resonance ($1s^2\ ^1S_0$–$1s2p\ ^1P_1$, at 40.2 Å) line emission from a laser-produced carbon plasma has been studied as a function of laser intensity. The optimum laser intensity is found to be $\approx 1.3\times 10^{12}$ W/cm$^2$ for the maximum emission of $3.2\times 10^{13}$ photons sr$^{-1}$ pulse$^{-1}$. Since this line lies in the water window spectral region, it has potential application in x-ray microscopic imaging of biological sample in wet condition. Theoretical calculation using corona model for the emission of this line is also carried out with appropriate ionization and radiative recombination rate coefficients.

**Keywords.** XUV spectroscopy; laser-produced plasmas, flat-field spectrograph, Nd : phosphate glass laser.

**PACS Nos 52.25.Jm; 52.50.Jm**

## 1. Introduction

Intense XUV soft x-ray emission from laser-produced plasma sources is currently of great interest for a variety of research investigations like inertial confinement fusion [1], XUV soft x-ray lasing [2], high order harmonic generation [3] and technological applications like soft x-ray lithography [4] and x-ray contact microscopy [5]. In microscopic application use of x-ray source in the 'water window' spectral region of 23 Å to 44 Å (corresponding to $K$ absorption edges of oxygen and carbon respectively) is particularly attractive as it permits a large relative contrast in absorption by protein and water molecules in a live biological sample. The main advantage of laser-produced x-ray source is that it allows 'flash' imaging which can be used to study time-dependent dynamic changes in living biological samples, having wider accessibility compared to synchrotron sources and is also economical. It is therefore important to determine optimum laser parameters such as laser intensity to achieve high x-ray conversion in the above spectral range. Whereas medium and high atomic number targets give a broad band spectrum which requires monochromation for scanning x-ray microscopy, lower atomic number target gives a quasi-monochromatic line spectrum that does not necessarily require monochromation. For better resolution and quantitative measurements, single line emission is favored rather than quasi-continuous emission. Majority of the earlier measurements [6,7] deal with the continuum radiation at the water window range, whereas few [8,9] studies are carried out to investigate the suitability of the target element producing intense discrete lines in the water window range. For instance, Diado *et al* [9] have studied the emission in water window range from various targets (C, Al, Ti, Cu, Mo) and found that the carbon lines are the most intense. However, the optimization of laser power for maximizing the emission of these lines has not drawn due attention. The x-ray conversion efficiencies can be increased using short wavelength lasers whereas the desired x-ray spectral component can be maximized by creating a plasma that is populated predominantly with the relevant ions, that is, by optimizing the laser intensity.

In this paper we optimize the laser intensity for maximum emission of the CV $1s^2\ {}^1S_0$–$1s2p\ {}^1P_1$, line at 40.2 Å (He-$\alpha$). This line is chosen because it is amply separated from its nearest strong line, viz. the Lyman-$\alpha$ ($1s\ {}^2S_{1/2}$–$2p\ {}^2P_{3/2}$ at 33.7 Å) and He-$\beta$ ($1s^2\ {}^1S_0$–$1s3p\ {}^1P_1$ at 35 Å) lines. This spectral separation is advantageous for choosing the He-$\alpha$ line from amongst these lines. Further, because of the closed shell structure of CV ion that emits He-$\alpha$ line, it is more stable than that of CVI ion that gives Ly-$\alpha$ line, making He-$\alpha$ line emission less susceptible to temperature change of the plasma that can occur due to shot-to-shot variation in laser intensity. Moreover, plasma is more transparent for He-$\alpha$ line than that of Ly-$\alpha$ line. The brightness of the line is estimated from absolute efficiency [10] of the flat field spectrograph for this line and the absolute calibration data [11] of the film used. Theoretical calculation using corona model [12] for the emission of this line is also carried out with appropriate ionization and radiative recombination rate coefficients and compared with the experimental observations.

## 2. Experimental setup

The experiment was performed using a 2 GW, 4 ns Nd : phosphate glass laser system. The measurements were carried out with a flat-field spectrograph designed and fabricated in-house and was described in detail in our earlier paper [13]. The schematic of the geometry of flat-field focussing is shown in figure 1. The experimental setup is shown in figure 2, depicting the mounting of the spectrograph on one of the demountable flanges of the laser-plasma interaction chamber that had an octagonal shape. The mounting of the spectrograph was at right angle to the target normal. The chamber was evacuated to a pressure of $10^{-5}$ torr. It may be pointed out here that, although line emission in this direction is smaller compared to that along the target normal, this may be of interest for applications because of less plasma debris. Briefly, the spectrograph is based on using a variable groove-spacing grating with nominal groove number of 1200 l/mm for achieving flat-field focussing [14]. The source-to-slit distance was 60 mm whereas slit-to-grating and grating-to-film distance

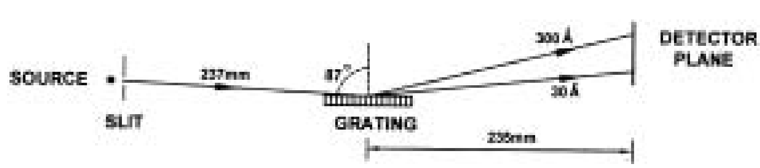


**Figure 1.** Schematic of the geometry of flat-field focussing.

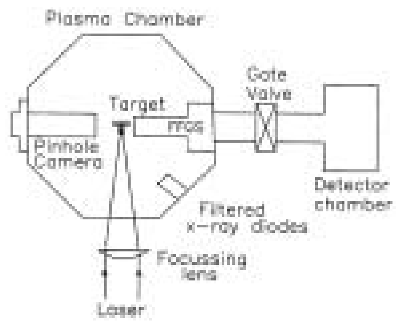


**Figure 2.** Experimental setup.

were 237 mm and 235 mm respectively. The width and height of the slit were 50 $\mu$m and 3 mm respectively.

The laser beam was focussed normally to the planar polyethylene(carbon) target using a 400 mm plano-convex lens. Laser shots of energy up to 5 J were fired on the target. The spectra were recorded on UFSh-4 Russian films and were developed in a D-19 developer for 6 min and fixed with standard acid fixer. Fresh target surface was used for each shot and all the spectra were recorded in a single shot exposure. Typical plasma source size as determined from an x-ray image (filtered through an aluminized 1 $\mu$m polycarbonate B-10 foil) recorded using a pinhole camera was $\approx$130 $\mu$m. Silicon PIN diodes (Quantrad 100 PIN-250) were also used for measuring integrated x-ray intensities filtered through B-10 foils.

## 3. Results and discussions

The densitometric trace of a carbon spectrum recorded on the film for a laser intensity of $\sim 7\times 10^{12}$ W cm$^{-2}$ is shown in figure 3. For different laser intensity shots, the optical density (and hence spectral line intensity) of the recorded spectral lines change which is shown in figure 4 for He-$\alpha$ line. The spectral lines are identified using standard data tables [15], and the transitions along with the ions are shown in figure 3. The lines are identified to be CV 1s$^2$ $^1S_0$–1s2p $^1P_1$ (He-$\alpha$) at 40.3 Å, CV 1s$^2$ $^1S_0$–1s3p $^1P_1$ (He-$\beta$) at 35.0 Å, CV 1s$^2$ $^1S_0$–1s4p $^1P_1$ (He-$\gamma$) at 33.4 Å, CV 1s$^2$ $^1S_0$–1s5p $^1P_1$ (He-$\delta$) at 32.8 Å, CV 1s$^2$ $^1S_0$–1s6p $^1P_1$ (He-$\varepsilon$) at 32.4 Å, CVI 1s $^2S_{1/2}$–2p $^2P_{3/2}$ (Ly-$\alpha$) at 33.7 Å. In this study, as discussed earlier, we will concentrate on the emission of He-$\alpha$ line from CV ions because this line at 40 Å is preferred as it is well-separated from the nearest intense Ly-$\alpha$ line (CVI 1s $^2S_{1/2}$–2p $^2P_{3/2}$) at 33.7 Å and He-$\beta$ (CV 1s$^2$ $^1S_0$–1s3p $^1P_1$) line at 35 Å.

For absolute spectral intensity estimation, calibration of the film sensitivity ($S_\lambda$) and contrast ratio $\gamma$ is required in addition to the absolute grating efficiency for the wavelength under consideration. Sensitivity ($S$) is defined as the inverse intensity in cm$^2$/erg needed to produce an optical density (OD) of 1.0 on the film and the contrast ratio $\gamma$ represents the slope of the optical density versus logarithmic exposure curve. The importance of film calibration lies in the fact that these parameters have significant dependence on radiation wavelength ($\lambda$). The data [11] on calibration of UFSh-4 film, using S-60 synchrotron radiation source at P.N. Lebedev Institute, is being used for our work.

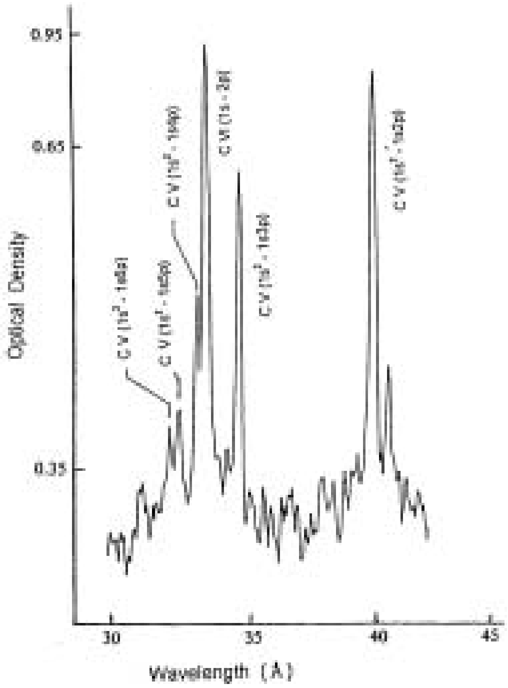


**Figure 3.** Spectrum of laser-produced carbon plasma.

The optical density values are converted to intensity ($I_\lambda$), using $\gamma$ value of the particular spectral line as $I_\lambda = 10^{\mathrm{OD}/\gamma(\lambda)}$. Then the absolute intensity is obtained [7] from the following equation:

$$I_{\lambda\,(\mathrm{absolute})} = I_\lambda [S_\lambda \eta_\lambda]^{-1} 10^{-1.0/\gamma(\lambda)}, \tag{1}$$

where $\eta_\lambda$ is the first-order diffraction efficiency of the grating. The factor $10^{-1.0/\gamma(\lambda)}$ appears in the above equation because the sensitivity values ($S_\lambda$) are defined in terms of inverse exposure required to obtain an optical density of 1.

Radiant energy per unit solid angle can then be calculated using the geometrical properties of the spectrograph whose slit subtends a solid angle of $4.2\times10^{-5}$ sr (slit height = 3 mm, slit width = 50 $\mu$m, source to slit distance = 60 mm). Absolute first-order efficiency of the He-$\alpha$ (40.2 Å) line for such a type of grating was measured to be $\eta_1 \approx 7.0 \times 10^{-3}$ by Schwanda *et al* [10]. Thus using the above equation the absolute intensity $I_{\lambda\,(\mathrm{absolute})}$ is estimated from the optical density of He-$\alpha$ line for different laser intensities and the result is plotted in figure 4. As seen from this figure, the photon flux first increases with increase in laser intensity, reaches a peak and then decreases. This is because, as the laser intensity increases the plasma temperature increases, hence the fractional abundance of He-like carbon ($C^{4+}$) ions (that emit He-$\alpha$ line) increases reaching a peak. With further increase in laser intensity the fractional abundance of this ion reduces, because at higher temperature plasma tends towards the fully ionized state leaving only bare ions. Also it is seen from the figure that the He-$\alpha$ emission is maximum for a laser intensity of $\approx 1.3 \times 10^{12}$ W/cm$^2$.

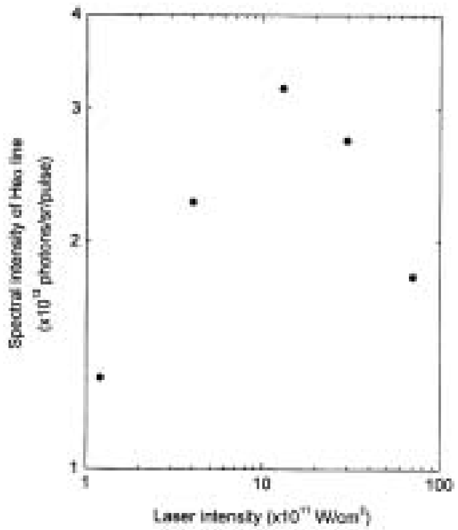


**Figure 4.** Experimentally measured variation of spectral intensity of He-$\alpha$ line with the variation of laser intensity.

At this laser intensity the emitted flux is $3.2 \times 10^{13}$ photons sr$^{-1}$ pulse$^{-1}$ and this corresponds to a dose of 1.6 mJ cm$^{-2}$ pulse$^{-1}$ and is reasonably good enough to give sufficient exposure required for microscopic applications [5]. It may be noted here that the accuracy of the spectral brightness estimated here is within $\pm 30\%$, and is determined primarily by the uncertainty in the film calibration data.

We have also theoretically investigated the variation of the intensity of this line with the variation of plasma temperature using a corona model that is satisfactorily applied to laser-produced plasma with electron density less than or equal to $10^{22}$ cm$^{-3}$ [12]. However, one may note here that several different formulations of collisional ionization ($S_{\rm coll}$) and radiative recombination ($\alpha$) rate coefficients have been published in the literature and are variously used by many workers for calculating the ion populations [12]. Since the theoretically calculated population density of an ionic charge state depends on the rate coefficients used, it is necessary to choose the combination of rate formulations that predict closest to the experimentally measured values. We have investigated this aspect and found that from amongst all the combinations of $S_{\rm coll}$ and $\alpha$, if the collisional ionization rate coefficient as formulated by Landshoff and Perez [16] along with the radiative recombination coefficient due to Pert [17] and dielectronic recombination coefficient due to Aldrovandi and Pequignot [18] is used, then the theoretical calculations are closest to the experimentally measured results of Galanti and Peacock [19] for the relative ion population of CVII to CVI ions for a laser-produced carbon plasma. Hence we will use the collisional ionization coefficient due to Landshoff and Perez ($S_{\rm coll}^{\rm LP}$), radiative recombination coefficient due to Pert ($\alpha^{\rm P}$) along with dielectronic recombination due to Aldrovandi and Pequignot ($\beta^{\rm AP}$).

The collisional ionization coefficient for an ionic charge state $Z$ due to Landshoff and Perez is given by

$$S_{\rm coll}^{\rm LP}(Z) = 1.24 \times 10^{-6} \xi_Z T_{eV}^{-3/2} [\exp(-u)/u^2] F_1(u) \quad {\rm cm}^3/{\rm s}, \qquad (2)$$

where $F_1(u) = 0.915(1+0.64)^{-2} + 0.42(1+0.5/u)^{-2}$, $u = \chi_Z/T_{eV}$, $\chi_Z$ = ionization potential in eV, $T_{eV}$ is the electron temperature, $\xi_Z$ is the number of electrons in the outermost $(n,l)$ subshell, $n$ and $l$ are the principle and azimuthal quantum numbers respectively. In the following, we write the radiative recombination coefficient $\alpha$ due to Pert for the ionic charge state $(Z+1)$ as

$$\alpha^{\mathrm{P}}(Z+1) = 5.2\times10^{-14}(Z+1)^4 T_{eV}^{-1/2} F_2(u) \quad \mathrm{cm}^3/\mathrm{s}, \tag{3}$$

where $F_2(u)$ is given as

$$\begin{aligned} F_2(u) &= \exp(u)(-\ln u - 0.5772 + u) \quad \text{for} \quad u \le 10^{-4} \\ &= \exp(u)(-\ln u - 0.5772 + 1.0u - 0.2499u^2 + 0.0552u^3 \\ &\quad -0.0098u^4 + 0.0011u^5) \quad \text{for} \quad 10^{-4} < u \le 1 \\ &= \frac{u + 2.3347 + 0.2506/u}{u^2 + 3.3307u + 1.6815} \quad \text{for} \quad u > 1. \end{aligned}$$

The formulation for dielectronic recombination $\beta$ as given by Aldrovandi and Pequignot [18] in the low electron density limit is as follows:

$$\beta^{\mathrm{AP}}(Z+1) = A_{\mathrm{di}} T_e^{-3/2} \exp(-T_0/T_e)[1 + B_{\mathrm{di}} \exp(-T_1/T_e)], \tag{4}$$

where $T_e$ is the electron temperature in K. The values of $A_{\mathrm{di}}$ (cm$^3$ s$^{-1}$ K$^{3/2}$), $B_{\mathrm{di}}$, $T_0$ (K) and $T_1$ (K) for all the carbon ions (except for CVII ions for which dielectronic recombination is not possible and hence $\beta = 0$) are taken from the above reference. The expression for line intensity ($P_{\mathrm{line}}$) is given by Griem [20] and used extensively by Colombant and Tonon [21] which is as follows:

$$P_{\mathrm{line}} = 7\times10^{-18} n_e n_{\mathrm{g}} T_{eV}^{-1/2} \sum_u f_{\mathrm{ug}} \exp(-E_{\mathrm{ug}}/T_{eV}), \tag{5}$$

where $n_e$ is the electron density and is taken to be $3\times10^{20}$ per cc, typical to the plasma under discussion, $n_{\mathrm{g}}$ is the ion density in the ground state (obtained using corona model) and is given by the product of fractional ion density with the total ion density, $f_{\mathrm{ug}}$ is the oscillator strength from upper level u to the ground state, and $E_{\mathrm{ug}}$ is the excitation energy from the ground state to level u. The atomic data tabulated by Wiese *et al* [22] are being used here.

The effect of opacity $\tau$ is accounted for by multiplying the transition probability (or oscillator strength) with the so-called 'escape factor' $G(\tau)$ to get the effective transition probability/oscillator strength. The escape factor is unity for optically thin lines and decreases rapidly with opacity. For the present case the opacity corresponding to a Doppler-broadened spectral line in a static plasma at the central wavelength is used and is as follows [20]:

$$\tau = 1.1\times10^{-16} \lambda n_{\mathrm{g}} l f_{\mathrm{gu}} \sqrt{\mu/kT_i}, \tag{6}$$

where $kT_i$ is the ion temperature in eV, $\lambda$ is the wavelength in Å of the concerned transition, $l$ is the path length through plasma in cm (taken as half of the plasma size, that is 65 $\mu$m for the present case), $f_{\mathrm{gu}}$ is the absorber oscillator strength of this transition, and $\mu \approx 2z$

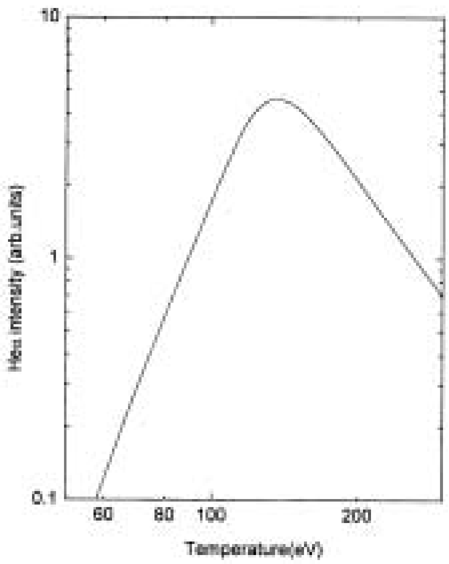


**Figure 5.** Theoretically calculated variation of spectral intensity of He-$\alpha$ line with the variation of electron temperature.

is the atomic mass number. For the calculation of opacity, $kT_i$ is approximated to $kT_e$ here [23]. The escape factor can be approximated to $G(\tau) \approx 1/\tau\sqrt{(\pi \ln \tau)}$ for $\tau \geq 2.5$ and $G(\tau) \approx \exp(-\tau/1.7)$ for $\tau < 2.5$ [24]. Theoretical calculations including opacity for line intensity of He-$\alpha$ line as a function of temperature is carried out using the above equation of line intensity and is plotted in figure 5. From the figure it is seen that the spectral intensity peaks at a temperature $\approx$130 eV. One may note here that the measured variation of He-$\alpha$ spectral line intensity as a function of laser intensity in figure 4 is similar to that of figure 5. This is because as the laser intensity increases the temperature of the plasma increases.

Plasma temperature was estimated corresponding to the emission peak using the technique of ratio of spectral line intensities. For this we have measured the intensity of He-$\beta$ line for the shot corresponding to a laser intensity of $1.3 \times 10^{12}$ W cm$^{-2}$ (laser intensity corresponding to the peak emission). The intensity ratio of He-$\alpha$ to He-$\beta$ lines for this laser intensity was measured to be 2.8. The plasma temperature of 120 eV was calculated theoretically using measured value of line intensity ratio (2.8) which was found in close agreement with plasma temperature of $\approx$130 eV corresponding to the peak emission as observed from figure 5. This is also in good agreement with the temperature $\approx$125 eV measured experimentally by Donaldson *et al* [25] for similar laser intensity for the same laser wavelength and a carbon target.

## 4. Conclusion

In summary we have optimized the intense emission of He-$\alpha$ line from a laser-produced carbon plasma with laser intensity using a grazing incidence flat-field spectrograph. Absolute measurements of this line emission is presented. Since this line lies in the water window spectral range it has potential application in x-ray microscopic imaging. The optimum emission flux of $1.3\times10^{13}$ photons/sr/pulse is measured for a laser intensity of $1.3\times10^{12}$ W cm$^{-2}$. The nature of variation of intensity of He-$\alpha$ line with plasma temperature calculated theoretically is found to be similar to that measured experimentally. Estimated plasma temperature based on measurement of line intensity ratio of He-$\alpha$ to He-$\beta$ shows that for the optimum emission the temperature of the plasma is 120 eV, which is in good agreement with the earlier observation of 125 eV reported in the literature.

**Acknowledgements**

The authors gratefully acknowledge J A Chakera, S Sailaja and V N Rai of Laser Plasma Division, CAT, Indore for various helpful discussions.

**References**

[1] J Lindl, *Phys. Plasmas* **2**, 3933 (1995)
[2] H Diado, *Rep. Prog. Phys.* **65**, 1513 (2002)
[3] R A Ganeev, J A Chakera, M Raghuramaiah, A K Sharma, P A Naik and P D Gupta, *Phys. Rev.* **A63**, 026402(1-6) (2001)
[4] M Chaker *et al*, *J. Vac. Sci. Technol.* **B10**, 3293 (1992)
[5] J Chakera, S R Kumbhare and P D Gupta, *J. X-ray Sci. Technol.* **8**, 1 (1998)
[6] K Eidmann and W Schwanda, *Laser and particle beams* **9**, 551 (1991)
[7] S Sailaja, P A Naik and P D Gupta, *IEEE Trans. Plasma Sci.* **29**, 960 (2001)
[8] M Kuhne and R Thornagel, *X-ray microscopy III, Springer series in optical sciences* edited by A Michette, G Morrison and C Backly (Springer-Verlag, Heidelberg, 1992) vol. 67, pp. 39–42
[9] H Diado, G M Zeng, T Tagawa, H Aritome, N Nakatsuka and S Nakai, *X-ray microscopy III, Springer series in optical sciences* edited by A Michette, G Morrison and C Backly (Springer-Verlag, Heidelberg, 1992) vol. 67, pp. 43–46
[10] W Schwanda, K Eidmann and M C Richardson, *J. X-ray Sci. Technol.* **4**, 8 (1993)
[11] Y M Alexandrov *et al*, *Nucl. Instrum. Methods Phys. Res.* **A308**, 343 (1991)
[12] G P Gupta and B K Sinha, *Phys. Rev.* **E56**, 2104 (1997)
[13] A Chowdhury, R A Joshi, S R Kumbhare, P A Naik and P D Gupta, *Sadhana* **24**, 557 (1999)
[14] T Kita, T Harada, N Nakano and H Kuroda, *Appl. Opt.* **22**, 512 (1983)
[15] R L Kelly and L J Palumbo, *Atomic and ionic emission lines below 2000 Å*. National Research Laboratory Report No. 7599 (Naval Research Laboratory, Washington DC, 1973)
[16] R K Landshoff and J D Perez, *Phys. Rev.* **A13**, 1619 (1976)
[17] G J Pert, *Laser Part. Beams* **12**, 209 (1994)
[18] S M V Aldrovandi and D Pequignot, *Astron. Astrophys.* **25**, 137 (1973)
[19] N Galanti and N J Peacock, *J. Phys.* **B8**, 2427 (1975)
[20] H Griem, *Plasma spectroscopy* (McGraw Hill, New York, 1964), p. 197
[21] D Colombant and G F Tonon, *J. Appl. Phys.* **44**, 3524 (1973)
[22] W L Wiese, M W Smith and B M Glennon, *Atomic transition probabilities* (US Department of Commerce Publication, 1966) vol. 1, NSRDS-NBS-4,
[23] R C Elton, *X-ray lasers* (Academic Press Inc., USA, 1990) p. 39
[24] T Holstein, *Phys. Rev.* **83**, 1159 (1951)
[25] T P Donaldson, R J Hutcheon and M H Key, *J. Phys.* **B6**, 1525 (1973)